

IN-64
9999
P. 17

Direct Replacement of Arbitrary Grid-Overlapping by Non-Structured Grid

Kai-Hsiung Kao
Institute for Computational Mechanics in Propulsion
Lewis Research Center
Cleveland, Ohio

and

Meng-Sing Liou
Lewis Research Center
Cleveland, Ohio

(NASA-TM-106601) DIRECT
REPLACEMENT OF ARBITRARY
GRID-OVERLAPPING BY NON-STRUCTURED
GRID (NASA. Lewis Research Center)
17 p

N94-33120

Unclass

G3/64 0009999

May 1994



National Aeronautics and
Space Administration



Direct Replacement of Arbitrary Grid-Overlapping by Non-Structured Grid

by

Kai-Hsiung Kao

*Institute for Computational Mechanics in Propulsion
NASA Lewis Research Center, Cleveland, OH 44135*

and

Meng-Sing Liou

*Internal Fluid Mechanics Division
NASA Lewis Research Center, Cleveland, OH 44135*

Abstract

A new approach that uses non-structured mesh to replace the arbitrarily overlapped structured regions of embedded grids is presented. The present methodology uses the Chimera composite overlapping mesh system so that the physical domain of the flowfield is subdivided into regions which can accommodate easily-generated grid for complex configuration. In addition, a Delaunay triangulation technique generates non-structured triangular mesh which wraps over the interconnecting region of embedded grids. It is designed that the present approach, termed DRAGON grid, has three important advantages: (1) eliminating some difficulties of the Chimera scheme, such as the orphan points and/or bad quality of interpolation stencils, (2) making grid communication in a fully conservative way, and (3) implementation into three dimensions is straightforward.

A computer code based on a time accurate, finite volume, high resolution scheme for solving the compressible Navier-Stokes equations has been further developed to include both the Chimera overset grid and the non-structured mesh schemes. For steady state problems, the local time stepping accelerates convergence based on a Courant-Friedrichs-Leury (CFL) number near the local stability limit. Numerical tests on representative steady and unsteady supersonic inviscid flows with strong shock waves are demonstrated.

I. Introduction

During the last decade both structured and unstructured grid systems have been developed and applied for the computations in various CFD problems. Among various grid concepts, there are currently two mainstream approaches for computing flow fields in which geometry imposes complex boundary conditions - composite structured grid schemes and unstructured grid schemes. In general, unstructured grid methods are considered to be more versatile and easier to adapt to complex geometry while composite structured grid methods are considered to use more efficient numerical algorithms and require less computer memory. However, both pure-strain approaches have their strengths and weaknesses.

The Chimera grid scheme¹ which uses overset grids to resolve complex geometry or flow features is generally classed into the composite structured grid category. Overset grids allow structured grids to be used without excessive distortion or inefficient use of grid density. It has been used to compute inviscid and high Reynolds flow about complex configurations,^{2,3} and even demonstrated for unsteady three dimensional viscous flow problems⁴ in which one body moves with respect to another. Overset grids have also been used as a solution adaptation procedure.^{5,6} It is found that the Chimera approach has more versatility than current unstructured schemes.

Up to date, the Chimera method is an outgrowth of trying to generalize a powerful solution approach to more complex situations. However, it is also recognized that there are weaknesses which must be removed if Chimera is to remain competitive with unstructured grids. There are two main criticisms leveled against the current implementations of the Chimera method: (1) the complexity of the interconnectivity is perhaps as difficult as dealing with an unstructured grid, many times resulting in orphan points and/or bad quality of interpolation stencils left in the computational domain, and (2) nonconservative interpolations to update interface boundaries are often used in practical cases. The fact that interpolation is generally used to connect grids implies that conservation is not strictly enforced. For some practical applications, such as the turbine-blade cooling passage flow in which heat transfer is involved and the supersonic inlet design where shock waves travel in time, the interpolation errors become overall-significant if numerical fluxes are not fully conserved.

It is remarked that while the space shuttle simulations have used simple interpolation procedures because of their robustness, Calspan/AEDC simulations have implemented an unpublished idea of Benek and use interpolants of delta quantities. Interpolating this quantity on interface boundaries ensures space-time conservation over the global field, but the penalty of this approach has not yet been rigorously examined (or clearly addressed). Many conservative interface schemes for overset grids have been devised.⁷⁻⁸ More recently, Wang and Yang⁹ transformed the conservation condition for overlapped grids to one of enforcing conservation for patched zones. However, a main drawback for those interface treatment methods is in determination of the area weights for irregular polygonal grid cells. Implementation into three dimensions is obviously difficult and not straightforward.

A fairly obvious way to ensure interface conservation would be to introduce an unstructured flow solver in the vicinity of the interface boundaries. Hybrid schemes which incorporate the best features of both structured and unstructured have already appeared¹⁰⁻¹¹ and will likely become more important in treating flow about complex geometries. In this paper a new approach is presented which uses non-structured mesh to replace the overset region for Chimera embedded grids. This approach not only eliminates the above criticisms but also preserves the advantages of the Chimera grid scheme. The extension of the present method to three dimensions is obviously

straightforward.

II. Structured and Unstructured Grid Schemes

Chimera Grid Scheme - Structured Grid System

The Chimera scheme is a grid embedding technique which provides a conceptually simple method for domain decomposition. For instance, a major grid is generated about a main body element and minor grids are then overset on the major grid so as to resolve interesting features of the configuration. Usually, the minor grids are overset on top of the major grid without requiring the mesh boundaries to join in any special way. However, a common or overlap region is always required to provide the means of matching the solutions across boundary interfaces. To increase the flexibility in the selection of subdomains, the Chimera scheme also allows an implementation to remove regions of a mesh containing an embedded grid from that mesh. That is, an embedded mesh introduces a "hole" into the mesh in which it is embedded. Typically, a hole is defined through a creation boundary which consists of a surface or a group of surfaces. The purpose of a hole creation boundary is to identify points that are within this boundary. A mesh point is considered to be inside a hole creation boundary if it is inside all surfaces that define the boundary. Figure 1 illustrates the connections between composite overlapping grids, with hole points being blanked by a prescribed creation boundary. Communication between overlaid grids is achieved by interpolation of boundary values from the mesh or meshes in which the boundaries are contained. For instance, the scheme employs nonconservative trilinear interpolation that as some simple experiments have shown is superior to Taylor series expansion. A practical application of the Chimera grid system for complete Space Shuttle/Solid Rocket Booster geometry is shown in Fig. 2. Details regarding the grid embedding technique can be found in Ref. 12.

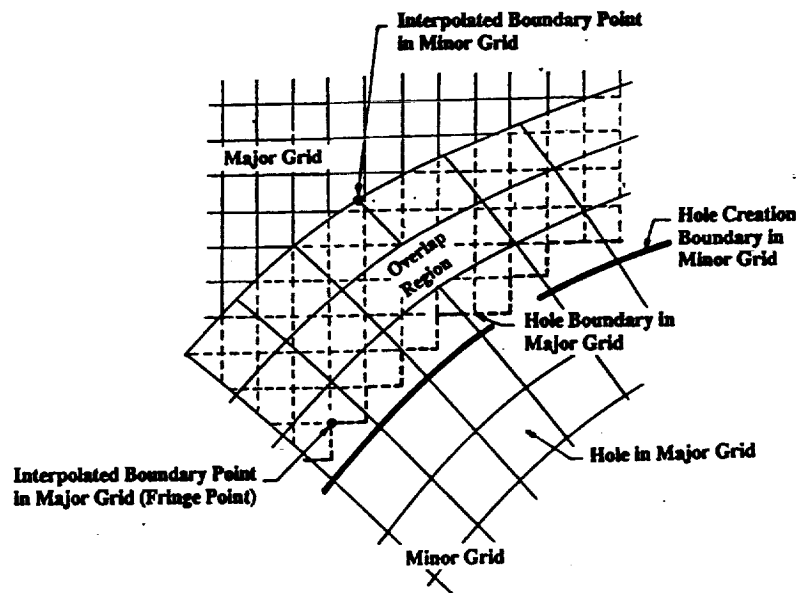


Figure 1. Interconnections of minor and major grids for Chimera overset grid scheme.
(Ref. 12)

A flow solver must be modified to account for the use of multiple meshes and the "hole" in the grids. These hole points must be blanked or excluded from the flow field solution. The main change in the flow algorithm itself is the treatment of the hole boundaries. The hole information from the Chimera grid package is stored in an array, IBLANK, which is defined for each point on each grid as

$$\text{IBLANK} = \begin{cases} 1, & \text{if a point is not blanked;} \\ 0, & \text{if a point is blanked.} \end{cases} \quad (1)$$

In the flow solver, each element in the corrector step is multiplied by the appropriate IBLANK value before the solutions are updated:

$$U^{n+1} = U^n + \text{IBLANK} \cdot (U^{n+1} - U^n) \quad (2)$$

The blanked solutions are updated in the interpolation routine. With this approach, no special routine or logic tests are required to exclude the blanked points from the flow field solution.

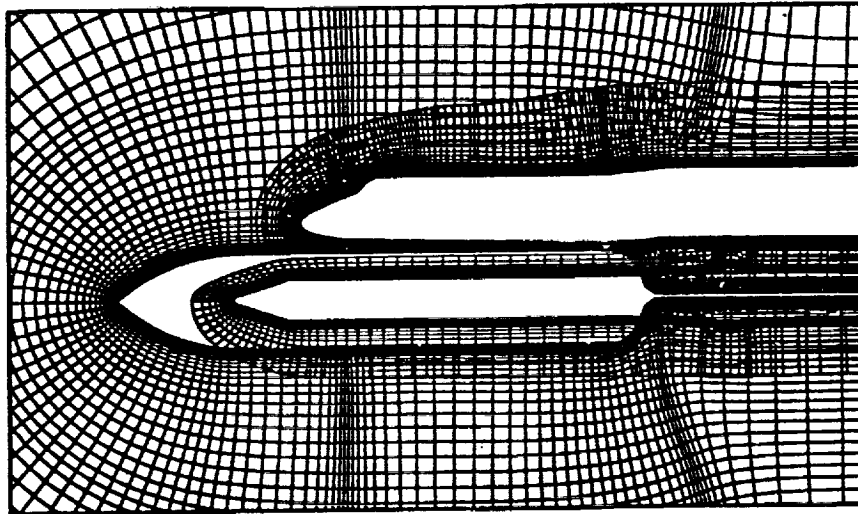


Figure 2. Overlapped grids for the Shuttle launch vehicle configuration. (Ref. 3)

DRAGON Grid - Hybrid Grid System

The application of the Chimera scheme involves two steps: (1) data communication between two embedded grids, and (2) execution of a flow solver that uses the communication information generated in step 1. The PEGSUS code is used to determine the interpolation coefficients between

composite grids. It is now modified to pursue the DRAGON grid technique. The approach of the DRAGON grid is accomplished by using non-structured mesh in the vicinity of the interface boundaries to replace the arbitrarily overlapped structured regions. Descriptions regarding the procedures to adopt the DRAGON grid method are summarized as follows:

- (1) The entire domain of a minor grid is used to form the hole creation boundary.
- (2) Grid points inside of the hole creation boundary are blanked out in the major grid.
- (3) Overset grid meshes are no longer exist. Instead, a new generated gap region is defined by the hole creation boundary as well as the hole boundary points. In result, interpolations of numerical fluxes or primitive quantities are no longer performed. (Fig. 3(a))
- (4) Both fringe points (hole boundary points) and interpolation boundary points are no longer treated as blanked points. Instead, they are now represented as interior points, and their IBLANK values are saved to be 1 in the PEGSUS code.
- (5) The fringe points as well as the boundary points are now forming the new boundaries for the unstructured grid generator. Details of unstructured grid generation will be addressed later in this section. A file named DRAGON is used for output of PEGSUS code which contains the boundary mesh coordinates of the unstructured region.

(6) Since interpolation process is not performed between structured grid blocks, output files providing interpolation information are deleted from the PEGSUS code.

It is known that the triangular shaped cell is the simplest geometric shape to cover a computational domain. A gap region created by arbitrary embedded grids implies an irregular shape of domain and would be very difficult to be represented by structured grids. The well-known Delaunay triangulation scheme¹³ is applied to perform the unstructured grid generation. The steps which adopt the triangular cells in combination with Chimera grid scheme are summarized.

- (1) Boundary nodes provided by the PEGSUS code are reordered according to their geometric coordinates.

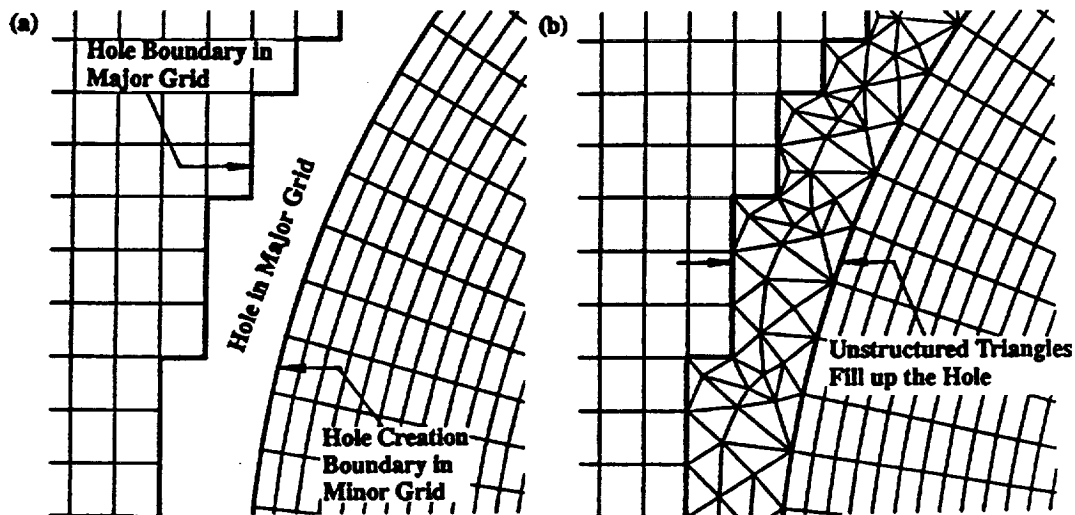


Figure 3. Direct replacement of arbitrary grid-overlapping by non-structured grid.

(a) Chimera grid method, (b) DRAGON grid method

(2) Delaunay triangulation method is then performed to connect the boundary nodes based on the Bowyer algorithm.¹⁴

(3) Triangles interior to bodies or exterior to the domain are deleted.

(4) Interior nodes are inserted in the circumcenter of triangles which are deemed to be too large based on the boundary spacing and a clustering parameter (which governs the rate of change of triangle area). This step completes the specification of the initial grid. (Fig. 3(b))

At present, no further grid inserting or deleting methods have been performed. Mesh improvement techniques, such as grid smoothing, aspect ratio control, equal length sides, etc., can be used to achieve better grid quality. An example of a coarse grid system about the multi-body domain by using the Delaunay triangulation method is shown in Fig. 4.

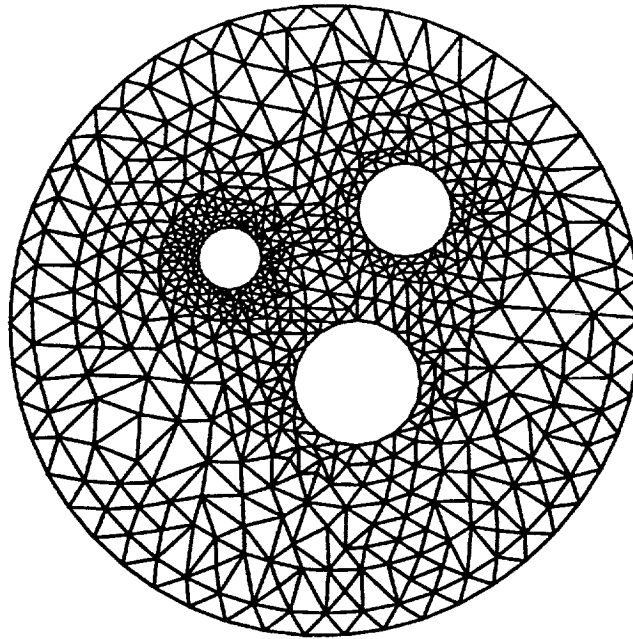


Figure 4. Delaunay triangular meshes for multi-body domain. (by Dr. James Loellbach)

With an unstructured grid, individual cells can no longer refer to their neighboring cells simply by using grid indices as in a structured grid. Instead, a connectivity matrix would be used to identify the relative position of the neighborhood of a cell. This connectivity matrix usually contains the cell based information as well as edge based information. With the present approach, connectivity matrices are also formed to define the discretized geometry between structured and unstructured grids. The connectivity matrices used in the present approach are summarized as following:

IEDGENODE(1:2, edges)
ICELLEGE(1:3, cells)
IEDGECCELL(1:2, edges)
IEDGETYPE(edges)
IEDGEFLUX(grids, edges)

- 2 nodes of each edge
- 3 edges of each triangular cell
- 2 neighboring cells of each edge
- edge type (type of boundary condition)
- edge number that connects structured and unstru-

IFLUXINDEX(grids, edges)

IFLUXINDY(grids, edges)

ctured grids

- i -index of structured cell that shares the edge fluxes with unstructured mesh

- j -index of structured cell that shares the edge fluxes with unstructured mesh

III. Governing Equations and Solver Algorithm

Governing Equations

Considering both structured and unstructured grid systems, the time-dependent compressible Euler equations can be expressed in an integral form in a volume v with enclosing surface s as follows

$$\int_v \frac{\partial U}{\partial t} dv + \oint_s \hat{n} ds \cdot F = 0 \quad (3)$$

where the conservative variable U is

$$U = [\rho, \rho \vec{u}, \rho E]^T \quad (4)$$

the inviscid flux F

$$F = [\rho \vec{u}, \rho \vec{u} \vec{u} + p \vec{I}, \rho H \vec{u}]^T \quad (5)$$

and the equation of state for ideal gas

$$p = (\gamma - 1) \rho e \quad (6)$$

Here e represents the internal energy. The vector quantities, expressed in terms of Cartesian coordinates, are denoted with an overhead arrow, and the tensor with an overhead tilde or a dyadic notation such as $\vec{u} \vec{u}$.

Flux Splitting

Based on the finite volume method, the governing equation is semi-discretized by assuming that the cell-centered conserved variables are constant within a cell, and that the flux integral at cell surface is also approximated by an average value of the numerical flux and the surface length. The numerical formulation uses a new class of flux splitting scheme. Accordingly, the name of the scheme is coined as Advection Upstream Splitting Method (AUSM).¹⁵ The scheme first splits the full flux into convective and pressure fluxes, $F_{1/2}^c$ and $F_{1/2}^p$ respectively,

$$F_{1/2} = F_{1/2}^c + F_{1/2}^p = c_{1/2} \Phi_{L/R} + P_{1/2} \quad (7)$$

at the cell interface $L < \frac{1}{2} < R$. The interface pressure, $P_{1/2}$, simply comprises the positive and negative data from appropriate domains of dependence via characteristic speed decomposition. The passive scalar variables $\Phi \equiv (\rho, \rho \tilde{u}, \rho H)$ is transported by a common convective velocity $c_{1/2}$ that is constructed in a similar fashion as $P_{1/2}$. Then the upwind idea is used to select the state, i.e., "L" or "R", of the variables to be convected. As such, the interface flux can be recast in the following form:

$$F_{1/2} = c_{1/2} \frac{1}{2} [\Phi_L + \Phi_R] - \frac{1}{2} |c_{1/2}| \Delta_{1/2} \Phi + P_{1/2} \quad (8)$$

where $\Delta_{1/2}(\) = (\)_R - (\)_L$. Here the first term on the right hand side is clearly not a simple average of the "L" and "R" fluxes, but rather a weighted average via the convective velocity.

Time Integration

An integration scheme assembles fluxes entering the cell interfaces and updates the conservative variables at the cell center. The present method originates from the Taylor series expansion in time, as was done in the Lax-Wendroff scheme. A two-step scheme with second order time accuracy is given as:

predictor:

$$U^* = U^n + \Delta t \frac{\partial U^n}{\partial t} \quad (9)$$

corrector:

$$U^{**} = U^* + \Delta t \frac{\partial U^*}{\partial t}$$

$$U^{n+1} = \frac{1}{2} (U^n + U^{**}) \quad (10)$$

The residual $\frac{\partial U}{\partial t}$ vanishes as the solution approaches a steady state. This scheme is restricted by the numerical stability condition. Note that both predictor and corrector steps are identical, with no need of defining a midpoint for the corrector step. This reduces the complexity of evaluating the transport terms in the general curvilinear coordinates.

Local Time Stepping

For steady state cases, local time stepping accelerates convergence to steady state by advancing the solution at each cell in time at a Courant-Friedricks-Leury (CFL) number near the local

stability limit. Thus, the expression for the local time step at each grid point (ξ, η, ζ) ,

$$\Delta t = CFL \cdot V / (|U| + a) S \quad (11)$$

where V is the cell volume, a is the local speed of sound, and S is the projected area in ξ, η , and ζ directions.

Data Communication Through Grid Interface

For multi-block grid system, the flow field is usually decomposed into separated regions according to different body geometry or flow features. However, the success of the overlaid grid or patched grid techniques relies on correct communication among grid blocks through boundary interfaces. Since the interface treatment methods are not necessarily satisfying any form of a conservative constraint, the solutions on overlaid grids are often mismatched with each other. This may result in instability or oscillations, especially when a shock wave passes through boundaries of overlaid grids.

In the current work, both the structured and unstructured flow solvers were based on a cell center scheme. The rectangles and triangles are the control volumes used in the finite volume formulation. Figure 5 illustrates the space discretizations of the volume cells for both structured and unstructured meshes. In the finite volume formulation (Eqn. 3), numerical fluxes will be evaluated at the cell interface based on the conditions of neighboring cells (L and R cells in Fig. 5). For unstructured grid, the edge flux, f_k , of the interface will be evaluated using the structured cell value as the right and the unstructured cell value as the left. On the other hand, for structured grid, the interface fluxes which have been evaluated in the unstructured process are applied directly in computation of the cell volume residuals, i.e. $f_{i+1/2,j} = f_k$. It is noted that no flux interpolation has been performed at any interface over the entire multi-block domain. Obviously, the present DRAGON grid approach automatically preserves both the local and global conservation law, and further implementation into three dimensions would be straightforward.

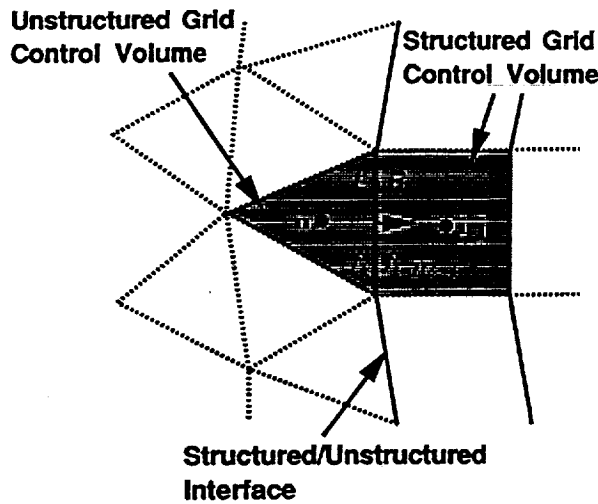


Figure 5. Control volumes for flux calculations.

IV. Tested Results and Discussion

Computational results are presented in this section for two-dimensional, inviscid, steady and unsteady problems. Test cases include supersonic flow past a circular cylinder and the shock tube problem. Numerical solutions have been obtained based on the following grid systems: (1) single grid, (2) Chimera grid, and (3) DRAGON grid. Integration of the equations of motion uses a first-order-accurate version of the flux splitting scheme in both structured and unstructured regions.

Case 1. Supersonic Flow over a Circular Cylinder

The first problem solved was that of a circular cylinder in a supersonic free stream ($M_\infty = 2.5$) with the associated bow shock. Three different mesh systems are employed. A single grid (Fig. 6(a)) with 61×51 points is first used to provide an analytic solution. The flow field is also resolved using Chimera overset grid scheme while the major grid (41×101) covers entire domain and the minor grid (61×31) wraps around the cylinder body. Figure 6(b) shows the overlaid meshes with hole points being blanked in the major grid. Nonconservative bi-linear interpolation method is used at the grid interface which allows fluid properties to communicate between the major and minor grids. With the DRAGON grid approach, the blanked hole is extended beyond the outer boundary of the minor grid, as shown in Fig. 6(c), and a new gap region is formed between two embedded grids. Delaunay triangulation method is then performed which generates triangular meshes to fill in this region (Fig. 6(d)). The new generated unstructured mesh includes 390 nodes and 616 triangular cells.

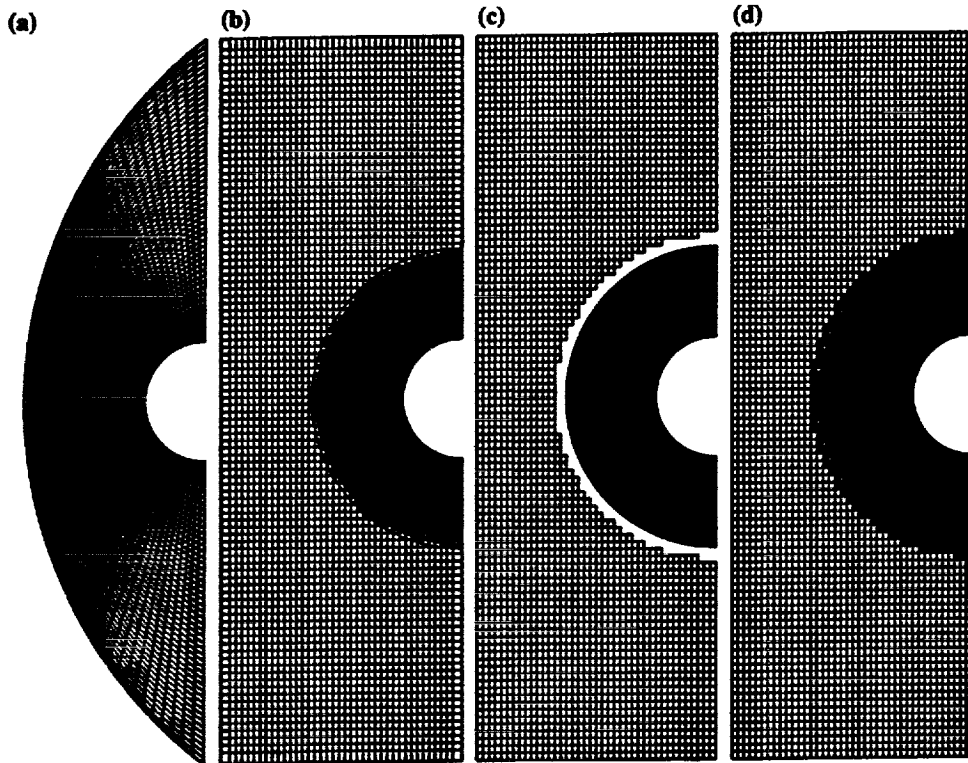


Figure 6. Computational grid systems for supersonic flow over circular cylinder.

($M_\infty = 2.5$)

(a) single grid, (b) Chimera grid, (c) hole points blanked in DRAGON grid,
(d) DRAGON grid

The values of the dependent variables at all the grid points are set equal to their free-stream values initially. The equations of motion with different grid systems are integrated until the solution converged to its steady-state value. Figure 7(a) shows the pressure contours obtained at convergence with the single grid mesh. Numerical solutions are also calculated based on both the Chimera grid and the DRAGON grid schemes, as displayed in Figs. 7(b) and 7(c) respectively, showing a comparable shock location to that predicted with the single grid system. The captured shock wave in Figs. 7(b) and 7(c) are seen to a slighter extent simply due to a coarser grid density. As noted in Fig. 7(b), both mismatched countour lines and pressure oscillations are observed in the vicinity of the grid interfaces.

For the DRAGON grid approach, both structured and unstructured results can be displayed on the same plot using the Flow Analysis Software Toolkit¹⁶ (FAST) visualization package on an IRIS workstation. As plotted in Fig. 7(c), the countour lines smoothly across the intersection boundaries; in fact, those lines seem to have a continuous slope across the interfaces. Note that small gaps interrupting the contour lines are observed along the interface boundaries as the cell center values are displayed in the structured grid region while unstructured grid values are plotted at their cell vertex locations.

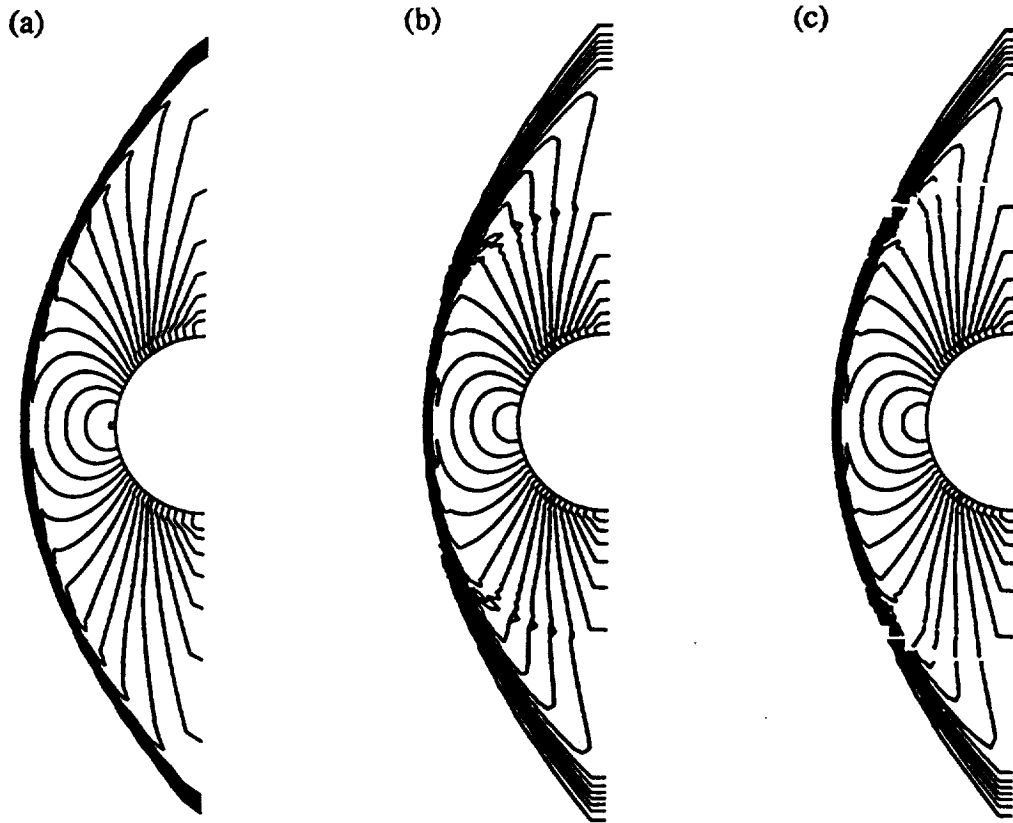


Figure 7. Pressure contours for supersonic flow over a circular cylinder. ($P_{min}=0.71$, $P_{max}=6.18$, $\Delta P=0.28$)
(a) single grid, (b) Chimera grid, and (c) DRAGON grid.

Figure 8 compares the pressure distributions along the centerline of the flow field. It is shown that, for this test problem, both Chimera and DRAGON grid methods perform very accurate prediction for shock location and strength.

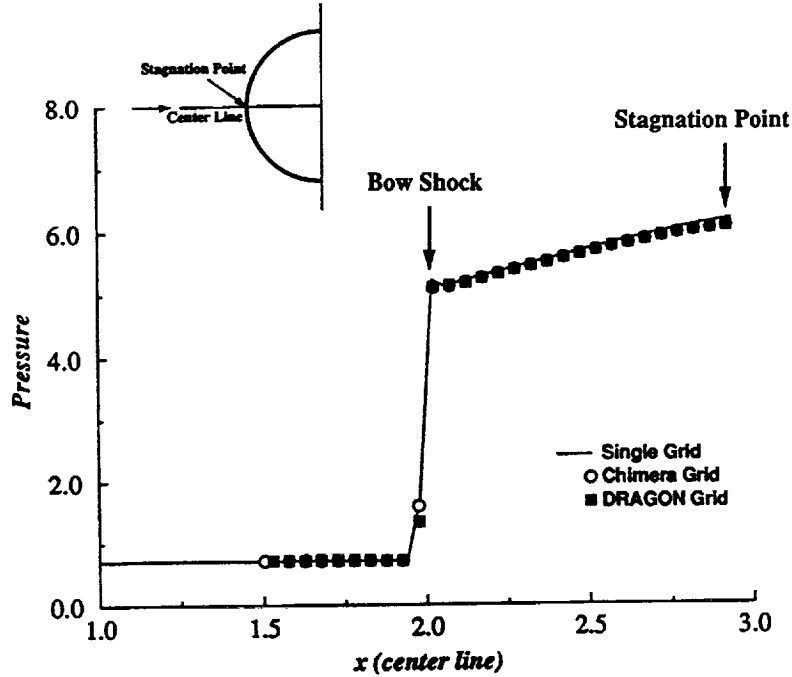


Figure 8. Pressure distributions along the centerline of the flow field. ($M_\infty = 2.5$)

Case 2. Shock Tube Problem

It is of great concern that inaccurate shock speed and strength may be captured if the numerical scheme is not fully conserved. An attempt is to test the time-dependent, plane moving shock problem on the embedded grid system. The shock wave is moving into a quiescent region in a constant-area channel with a designed shock speed $M_s = 4$. Like the first test case, the computational domain is composed using the single grid, the Chimera grid as well as the DRAGON grid schemes. As shown in Fig. 9(a), the single grid system containing a grid dimension of 801×21 is used to provide an analytic solution for shock location. Figure 9(b) illustrates the Chimera grid system which includes a major grid (upstream region) of size 41×21 , and a minor grid (downstream region) of dimension 781×21 . The grid lines between two overlaid grids are embedded in any arbitrary orientation. Upon the replacement of grid-overlapping by non-structured grid, the DRAGON grid for the moving shock problem is shown in Fig. 9(c). Note that all three grid systems apply equivalent grid densities in the overall regions, except for that near the interface boundaries.

It is designed that the initial shock position is marked in the upstream region. (Fig. 9) The initial conditions for the flow field are assumed to have the left and right values as

$$\begin{array}{ccc}
 \rho_L = 4.57 & \longrightarrow & \rho_R = 1 \\
 P_L = 13.21 & & P_R = 0.71 \\
 u_L = 3.125 & & u_R = 0 \\
 v_L = 0 & & v_R = 0
 \end{array}$$

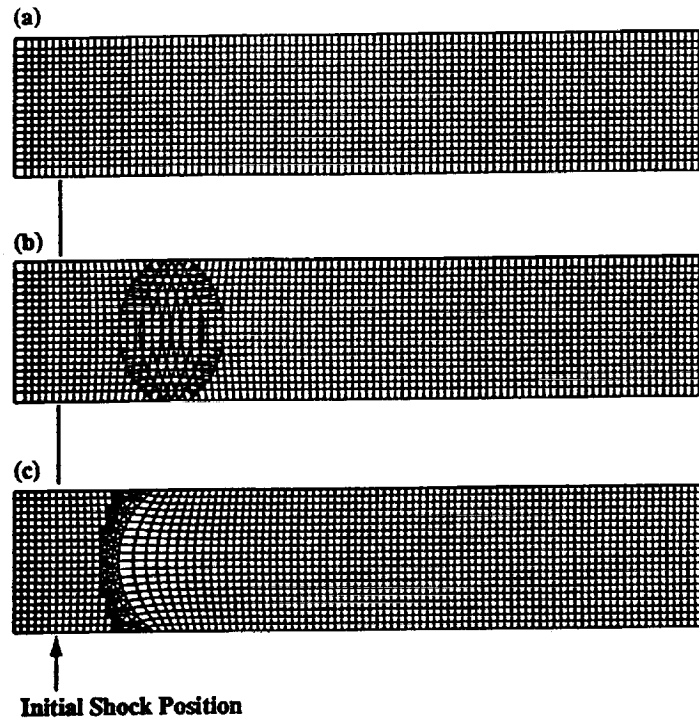


Figure 9. Computational grid systems for moving shock problem. ($M_s = 4$)
 (a) single grid, (b) Chimera grid, and (c) DRAGON grid.

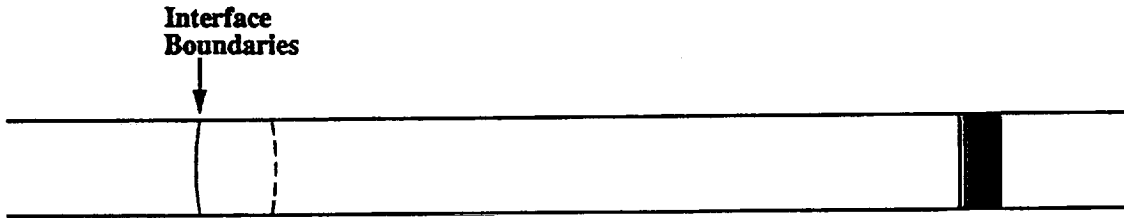


Figure 10. Pressure contours for moving shock problem. (500 iterations, $\Delta t=0.1$)

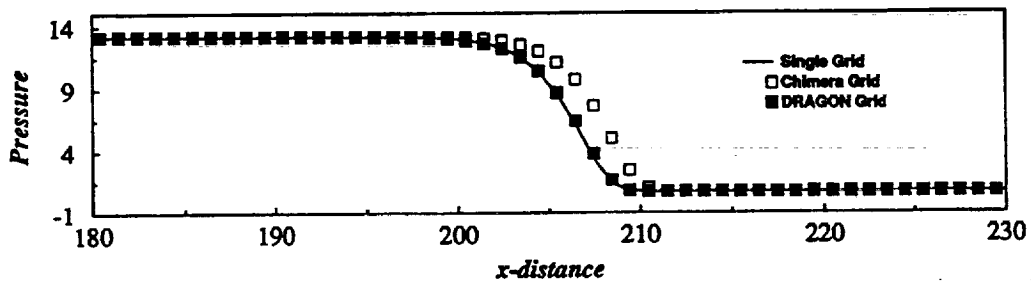


Figure 11. Comparison of pressure distributions along the centerline of the channel.

Figure 10 displays the pressure contours with various grid systems at a downstream location after the shock wave passing through the interface boundaries. It is hardly to identify any difference on the contour lines between three grid systems. However, a critical comparison of the pressure distributions along the centerline of the channel, as plotted in Fig. 11, shows that the Chimera scheme predicts a faster moving shock in the tube. As a result, the present DRAGON grid approach accurately captures the shock speed which ensures the numerical solution is preserved in a fully conservative nature.

V. Conclusion

In this paper we presented a new approach, termed the DRAGON grid, that uses non-structured mesh to replace the arbitrarily overlapped structured regions of embedded grids. It is designed to further enhance the flexibility for Chimera overlapping grid technique and to enforce conservative grid communication between embedded grids. Numerical results obtained for steady and unsteady problems indicated that the fluid properties have been accurately carried through the interface boundaries. Future plans include unstructured grid improving and 3D implementation of the DRAGON grid are now ongoing and will soon be reported.

Acknowledgements

The first author would like to thank Dr. James Loellbach for his valuable discussions and providing the main coding structures for Delaunay triangulation and the unstructured flow solver. The computational results for the test problems are obtained using the CRAY-YMP computer system at NASA Lewis Research Center and partly calculated on the C90 at NASA Ames Research Center.

References

- ¹Benek, J. A., Buning, P. G. and Steger, J. L., "A 3-D Chimera Grid Embedding Technique," AIAA Paper 85-1523, 1985.
- ²Steger, J. L. and Benek, J. A., "On the Use of Composite Grid Schemes in Computational Aerodynamics," *Comp. Methods Appl. Mech. and Eng.*, Vol. 64, Nos. 1-3, 1987.
- ³NASA Ames Space Shuttle Flow Simulation Group: P. G. Buning, I. T. Chiu, F. W. Martin Jr., R. L. Meakin, S. Obayashi, Y. M. Rizk, J. L. Steger and M. Yarrow, "Flowfield Simulation of the Space Shuttle Vehicle in ascent," *Proceedings of the Fourth International Conference on Supercomputing*, Santa Clara, CA, (1989).
- ⁴Meakin, R. L. and Suhs, N., "Unsteady Aerodynamic Simulation of Multiple Bodies in Relative Motion," AIAA 9th Computational Fluid Dynamics Conference.
- ⁵Kao, K. H., Liou, M. S. and Chow, C. Y., "Grid Adaptation Using Chimera Composite Overlapping Meshes," AIAA Paper 93-3389, Orlando, FL, July 1993.
- ⁶Berger, M. J. and Oliger, J., "Adaptive Mesh Refinements for Hyperbolic Partial Differential Equations," *J. Comp. Physics*, Vol. 53, 1987.
- ⁷Merger, M. J., "On Conservation at Grid Interfaces," ICASE Report 84-43, NASA Langley Research Center, Hampton, Virginia, 1984.
- ⁸Moon, Y. J. and Liou, M.-S., "Conservative Treatment of Boundary Interfaces for Overlaid

Grids and Multi-level Grid Adaptations," AIAA Paper 89-1980-CP, 1989.

⁹Wang, Z. J. and Yang, H. Q., "A Unified Conservative Zonal Interface Treatment for Arbitrarily Patched and Overlapped Grids," AIAA Paper 94-0320, January 1994.

¹⁰Nakahashi, K., "FDM-FEM Zonal Approach for Computations of Compressible Viscous Flows," 10th International Conference on Numerical Methods in Fluid Dynamics, Beijing, China, June, 1986.

¹¹Soetrisno, M., Imlay, S. T. and Roberts, D. W., "A Zonal Implicit Procedure for Hybrid Structured-Unstructured Grids," AIAA Paper 94-0645, January 1994.

¹²Suhs, N. E. and Tramel, R. W., "PEGSUS 4.0 User's Manual," AEDC-TR-91-8, Calspan Corporation/AEDC Operations, November 1991.

¹³Hase, J. E., Anderson, D. A. and Parpia, I., "A Delaunay Triangulation Method and Euler Solver for Bodies in Relative Motion," AIAA-91-1590-CP, Hawaii, June 1991.

¹⁴Bowyer, A., "Computing Dirichlet Tessellations," The Computer J., Vol. 24, No. 2, pp. 162-166, 1981.

¹⁵Liou, M. S., "On a New Class of Flux Splitting," 13th International Conference on Numerical Methods for Fluid Dynamics, Rome, Italy, July 1992.

¹⁶Walatka, P. P., Clucas, J., McCabe, R. K., Plessel, T. and Potter, R., "FAST User Guide," NASA Ames Research Center, RND-93-010, July 1993.

REPORT DOCUMENTATION PAGE			Form Approved OMB No. 0704-0188	
Public reporting burden for this collection of information is estimated to average 1 hour per response, including the time for reviewing instructions, searching existing data sources, gathering and maintaining the data needed, and completing and reviewing the collection of information. Send comments regarding this burden estimate or any other aspect of this collection of information, including suggestions for reducing this burden, to Washington Headquarters Services, Directorate for Information Operations and Reports, 1215 Jefferson Davis Highway, Suite 1204, Arlington, VA 22202-4302, and to the Office of Management and Budget, Paperwork Reduction Project (0704-0188), Washington, DC 20503.				
1. AGENCY USE ONLY (Leave blank)		2. REPORT DATE May 1994		3. REPORT TYPE AND DATES COVERED Technical Memorandum
4. TITLE AND SUBTITLE Direct Replacement of Arbitrary Grid-Overlapping by Non-Structured Grid			5. FUNDING NUMBERS WU-505-90-5K	
6. AUTHOR(S) Kai-Hsiung Kao and Meng-Sing Liou				
7. PERFORMING ORGANIZATION NAME(S) AND ADDRESS(ES) National Aeronautics and Space Administration Lewis Research Center Cleveland, Ohio 44135-3191			8. PERFORMING ORGANIZATION REPORT NUMBER E-8875	
9. SPONSORING/MONITORING AGENCY NAME(S) AND ADDRESS(ES) National Aeronautics and Space Administration Washington, D.C. 20546-0001			10. SPONSORING/MONITORING AGENCY REPORT NUMBER NASA TM-106601 ICOMP-94-7	
11. SUPPLEMENTARY NOTES Meng-Sing Liou, NASA Lewis Research Center and Kai-Hsiung Kao, Institute for Computational Mechanics in Propulsion (work funded by NASA Cooperative Agreement NCC3-233). ICOMP Program Director, Louis A. Povinelli, organization code 2600, (216) 433-5818.				
12a. DISTRIBUTION/AVAILABILITY STATEMENT Unclassified - Unlimited Subject Category 64			12b. DISTRIBUTION CODE	
13. ABSTRACT (Maximum 200 words) A new approach that uses non-structured mesh to replace the arbitrarily overlapped structured regions of embedded grids is presented. The present methodology uses the Chimera composite overlapping mesh system so that the physical domain of the flowfield is subdivided into regions which can accommodate easily-generated grid for complex configuration. In addition, a Delaunay triangulation technique generates non-structured triangular mesh which wraps over the interconnecting region of embedded grids. It is designed that the present approach, termed DRAGON grid, has three important advantages: (1) eliminating some difficulties of the Chimera scheme, such as the orphan points and/or bad quality of interpolation stencils, (2) making grid communication in a fully conservative way, and (3) implementation into three dimensions is straightforward. A computer code based on a time accurate, finite volume, high resolution scheme for solving the compressible Navier-Stokes equations has been further developed to include both the Chimera overset grid and the non-structured mesh schemes. For steady state problems, the local time stepping accelerates convergence based on a Courant-Friedrichs-Leury (CFL) number near the local stability limit. Numerical tests on representative steady and unsteady supersonic inviscid flows with strong shock waves are demonstrated.				
14. SUBJECT TERMS Overset grid; Hybrid grid; Supersonic flow			15. NUMBER OF PAGES 17	
			16. PRICE CODE A03	
17. SECURITY CLASSIFICATION OF REPORT Unclassified	18. SECURITY CLASSIFICATION OF THIS PAGE Unclassified	19. SECURITY CLASSIFICATION OF ABSTRACT Unclassified	20. LIMITATION OF ABSTRACT	